http://dx.doi.org/10.5012/bkcs.2012.33.3.809

Study of the Resonance Structures of the Preionizing Spectrum of Molecular Hydrogen by Phase-shifted Multichannel Quantum Defect Theory†

Chun-Woo Lee

Center for Space-Time Molecular Dynamics, Seoul National University, Seoul 151-747, Korea
Department of Chemistry, Ajou University, Suwon 443-749, Korea. E-mail: clee@ajou.ac.kr
Received September 26, 2011, Accepted December 5, 2011

The resonance structure of the preionization spectrum of H_2 in the region immediately above its H_2^+ ionization threshold, ($^2\Sigma_g^+$, ν^+=0, N^+=0) converging toward its rotationally excited (ν^+=0, N^+=2) limit, is complicated due to perturbation by the vibrationally excited levels 7pπ v = 1 and 5pπ v = 2. The spectra of interlopers are separated from the rotationally preionizing Rydberg series to allow analysis of this complex resonance structure. Although only two vibrationally excited levels perturb the rotational preionization spectrum, at least 6 interloper Rydberg series participate in the complex spectrum over most of its energy range and more interloper series participate at a narrow range around 124500 cm^{-1} in the spectrum. To allow handling of an arbitrary number of interloper series, MATLAB®'s symbolic operation is used to perform on-the-fly formulation.

Key Words : Phase-shifted MQDT, Overlapping resonances, Preionization of H_2, Interlopers

Introduction

Autoionization spectra frequently show complex overlapping resonances caused by interlopers. Multichannel quantum defect theory (MQDT) is a powerful tool used to model such complex resonances using only a few parameters.[1] However, resonance structures are not transparently identified in its formulation because of its indirect treatment of resonances. To exhibit resonance behaviours transparently, phase-shifted base pairs were introduced to MQDT by Giusti-Suzor and Fano,[2] although their utility has been limited because of the complicated transformations in multi-closed-channel systems.[3] Instead, observed spectra have been reproduced by acquiring the minimum required MQDT parameters. For autoionizing series perturbed by interlopers, there is no need to perform all the mathematical transformations to identify the resonance structures. Outline resonance structures are acquired using physical simplifications holding for such perturbed series. The remaining derivation is normally much simpler, as first introduced by Cooke and Cromer[4] through the use of phase-shifted MQDT. Their treatment was translated into a simple mathematical form by Ueda.[5] This MQDT formulation is equivalent to the theory used for Rydberg series of discrete levels coupled with a continuum of finite bandwidth, originally explored by Cohen-Tannoudji and Avan and adapted for autoionization by Connerade.[6] The latter treatment was developed further by Lane[7] in the framework of Fano and Cooper's theory.[8]

In previous studies,[9,10] Ueda's simple mathematical formulation was extended to a system of 3 closed channels involving two interacting autoionizing Rydberg series perturbed by an interloper. Formulas for the changes in resonance structures caused by the channel coupling of two autoionizing Rydberg series under perturbation by an interloper were obtained and applied to the experimental data reported in Refs. [11] and [12]. This work continues these previous studies of analysing resonance structures in complex spectra by decoupling the interloper's spectrum from the autoionizing Rydberg series. Decoupling is attempted here for the complex spectra shown by H_2 molecules,[13] which involve several mutually coupled interlopers.

Unlike the case of atomic autoionization spectra, application of phase-shifted MQDT to molecular autoionization spectra is rare, with the primitive analysis by Giusti-Suzor and Lefebvre-Brion[14] being the only published report. Their work did not incorporate the advantages that the frame transformation matrix version of MQDT[15] provides, such as the available eigenframes in the short- and long-ranges, the physical simplifications of the dynamics holding for the Born-Oppenheimer states, and its intrinsic capability to include non-adiabatic interactions,[16] the very nature of fragmentation channels. The photoionization spectrum of H_2 in the region immediately above the threshold of its ionization to $H_2^+(^2\Sigma_g^+,\ v^+=0,\ N^+=0)$ converging towards its rotationally excited ($v^+=0,\ N^+=2$) limit studied by Jungen and Dill[17] was chosen as the system for which the phase-shifted formulation of multichannel quantum defect theory was developed. The study of Jungen and Dill remains one of the most accurate and extensive studies despite there being many subsequent relevant studies of hydrogen molecules,[18-22] including work from the same group.[23,24] Their study was used for the coherent control of the outcomes of chemical reactions, in particular the control of the branching ratio of photoionization and photodissociation by optical pulse trains. Kirrander, Jungen, and Fielding[25]

†This paper is to commemorate Professor Kook Joe Shin's honourable retirement.

showed that the coherent control is determined by the overlap between the spectral profile of the pulse train and the molecular spectrum, in particular the resonance structures of the spectrum. Therefore for the control of chemical reactions, control of the photoionization spectrum should be performed in advance and in this respect, the capability of phase-shifted MQDT to show resonance structures transparently so as to facilitate the control of photoionization spectra will be useful in controlling photo-processes.

System

The practical use of MQDT with atomic systems generally involves phase-shifted MQDT[2] beginning directly from either zero sub-matrices or zero diagonal sub-matrices depending on the system. Consider a system of 3 closed channels, with two perturbers perturbing one closed channel (Fig. 1). Let the number of open channels be limited to one. Let the closed channels be indexed by 1, 2, and 3 and the open channel by 4. The ionization thresholds, I_i, are taken to satisfy $I_3 \geq I_2 >> I_1 > I_4$. For such systems, the open-open part K^{oo} and the diagonal elements of the closed-closed part K^{cc} of the short-range reactance matrix K can be set to zero by phase renormalization.[5,26] With the tilde emphasizing phase shift, the phase-shifted reactance matrix is given as follows:

$$\tilde{K}=\begin{pmatrix} 0 & \tilde{K}_{12} & \tilde{K}_{13} & \tilde{K}_{14} \\ \tilde{K}_{12} & 0 & \tilde{K}_{23} & \tilde{K}_{24} \\ \tilde{K}_{13} & \tilde{K}_{23} & 0 & \tilde{K}_{34} \\ \tilde{K}_{14} & \tilde{K}_{24} & \tilde{K}_{34} & 0 \end{pmatrix}=\begin{pmatrix} \tilde{K}^{cc} & \tilde{K}^{co} \\ \tilde{K}^{oc} & \tilde{K}^{oo} \end{pmatrix} \quad (1)$$

It is convenient to introduce a coupling parameter $\tilde{\xi}_i$ (i = 1, 2, 3) for the reactance matrix elements $\tilde{K}_{4i}^{oc}$ between the open and closed channels. Its square $\tilde{\xi}_i^2$ is related to the spectral width $\tilde{\Gamma}_i$ of the resonance peak of an autoionizing series i as $\tilde{\Gamma}_i = 4\text{Ryd}\,\tilde{\xi}_i^2/\pi\nu_i^3$,[2] where Ryd denotes the Rydberg constant and ν_i denotes the effective quantum number defined by $E = I_i - \text{Ryd}/\nu_i^2$ for channel i. $\tilde{W}_i$ denotes $\tilde{\xi}_i^2$:

$$\tilde{W}_i = \tilde{\xi}_i^2 = \tilde{K}_{4i}^2 \quad (2)$$

For molecular systems, the frame-transformation version of MQDT is generally used.[18] The reactance matrices are not of the form of Eq. (1). To use phase-shifted MQDT, the reactance matrices should be transformed into the form of (1) by shifting the phases of the channel basis wavefunctions. Phase shifts $\mu = [\mu^c\ \mu^o]$ that transform reactance matrices to the form of (1) can be obtained by solving the coupled equations as follows[27]

$$\tilde{K}_{ii}^{cc}=[(K'^{cc}\sin\pi\mu^c+\cos\pi\mu^c)^{-1}(K'^{cc}\cos\pi\mu^c-\sin\pi\mu^c)]_{ii}=0 \quad (3)$$

where K'^{cc} is defined by

$$K'^{cc}=K^{cc}-K^{co}\sin\pi\mu^o(K^{oo}\sin\pi\mu^o+\cos\pi\mu^o)^{-1}K^{oc} \quad (4)$$

A similar equation holds for $\tilde{K}^{oo}$ as follows:

$$\tilde{K}_{ii}^{oo}=[(K'^{oo}\sin\pi\mu^o+\cos\pi\mu^o)^{-1}(K'^{oo}\cos\pi\mu^o-\sin\pi\mu^o)]_{ii}=0 \quad (5)$$

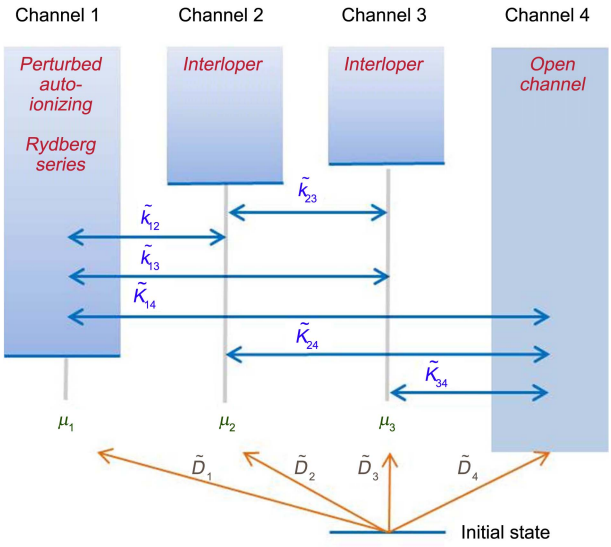

Figure 1. The channel structure of a system comprising three closed and one open channel. $\tilde{K}_{ij}$ denotes the short-range reactance matrix elements and $\tilde{k}_{ij}$ denotes $\tilde{K}_{ij}/(\tilde{\xi}_i\tilde{\xi}_j)$ with $\tilde{\xi}_i$ defined in (2). $\tilde{D}_i$ is the transition dipole moment to channel i and $\tilde{\mu}_i$ denotes the phase shift to make the reactance matrix into the form of (1).

with

$$K'^{oo}=K^{oo}-K^{oc}\sin\pi\mu^c(K^{cc}\sin\pi\mu^c+\cos\pi\mu^c)^{-1}K^{co} \quad (6)$$

The photoionization spectrum of molecular hydrogen has more than 2 interloper series participating in the photoionization. To model this, the number of interloper series should be extended to any arbitrary number. Since the extension follows the same procedure as that for the four channel system in Figure 1, first presented is the formulation for the four channel system, for which the reactance matrix is given by Eq. (1). Its extension to include arbitrary numbers of interloper series is presented later.

Photoionization Cross Section

Photoionization cross sections can be calculated from $\sigma = (4\pi^2\alpha\omega/3)|\mathbf{D}|^2$ with ω the wave-number of an absorbed photon, α the fine-structure constant and $\mathbf{D}$ the transition dipole moment $(\Psi|T|i)$ from the initial state i to the final energy-normalized autoionizing eigenfunctionΨ.[3] In phase-shifted MQDT, Ψ will be denoted with a tilde as $\tilde{\Psi}$. The formula can be expanded in terms of the real standing-wave channel basis functions in matrix form as:

$$\tilde{\Psi}=\tilde{\Psi}^o\cos\tilde{\delta}-\tilde{\Psi}^c(\tilde{K}^{cc}+\tan\tilde{\beta})^{-1}\tilde{K}^{co}\cos\tilde{\delta} \quad (7)$$

where $\tilde{\Psi}^c$ represents the column vector composed of standing wave closed-channel-basis functions $\tilde{\Psi}_i$ with running indices i = 1, 2, and 3 for the system in Figure 1 and $\tilde{\Psi}^o$ is the open channel standing wave channel basis function and is equal to $\tilde{\Psi}_4$. The standing wave channel basis functions are defined elsewhere.[2] $\tilde{\beta}_i$ in (7) denotes phase shifted $\beta_i(\equiv\pi\nu_i)$ by, $\pi\mu_i$, i.e., $\tilde{\beta}_i=\pi(\nu_i+\mu_i)$ where ν_i is the effective

quantum number defined in Eq. (2). The factor $\cos\tilde{\delta}$ in (7), which is equal to $(1+\tilde{\mathbf{K}}^2)^{-1/2}$, is needed to compensate for the energy non-normalized $\tilde{\Psi}_i$ to make $\tilde{\Psi}$ energy-normalized. In the phase-shifted representation, where $\tilde{K}^{oo}$ is null, the background phase shift $\tilde{\delta}_0$ is zero, whereby $\tilde{\delta}$ is equal to $\tilde{\delta}_r$.[28] The resonance phase shift $\tilde{\delta}_r$ can be conveniently obtained from the phase of $\det(\tan\tilde{\beta}+\tilde{\kappa}^{cc})$ (see Eq. (14) of Ref. [29]), where the complex reactance matrix $\tilde{\kappa}^{cc}$ denotes $\tilde{K}^{cc}-i\tilde{K}^{co}\tilde{K}^{oc}$, first considered in Ref. [26].

Closed channels with higher ionization limits frequently act as interlopers, providing broad background peaks to the autoionizing series converging to the lowest ionization limit of the closed channels. The influence of single interlopers on the convergence of autoionization Rydberg series to lower ionization limits has been examined by Connerade,[6] Lane,[7] Cooke and Cromer,[4] and Ueda.[5] An interloper has negligible influence from the autoionizing Rydberg series as its spectral width is normally much broader than that of the perturbed autoionizing series and it ionizes too quickly to be affected by a perturbed series. According to this physical argument, cross sections can be decoupled into those of an interloper and of an autoionizing series perturbed by an interloper:

$$\sigma_{res}=K(\tilde{D}^o)^2\frac{(\tilde{\varepsilon}_2+\tilde{q}_2)^2}{\tilde{\varepsilon}_2^2+1}\frac{(\tilde{\varepsilon}_{1eff}+\tilde{q}_{1eff})^2}{\tilde{\varepsilon}_{1eff}^2+1}\equiv\tilde{\sigma}_{interloper}\frac{(\tilde{\varepsilon}_{1eff}+\tilde{q}_{1eff})^2}{\tilde{\varepsilon}_{1eff}^2+1}, \quad (8)$$

as obtained by Ueda,[5] where K enotes $4\pi^2\alpha\omega/3$, $\tilde{D}^o$ denotes the transition dipole moment to the open channel. In (8), $\tilde{\varepsilon}_2$ and $\tilde{q}_2$ denote the reduced energy and line profile index, respectively, for series 2 acting as an interloper and are defined as

$$\tilde{\varepsilon}_2=\frac{\tan\pi(\nu_2+\mu_2)}{\tilde{W}_2}=\frac{\tan\tilde{\beta}_2}{\tilde{W}_2}$$

$$\tilde{q}_2=-\frac{\tilde{D}_2}{\tilde{\xi}_2\tilde{D}^o} \quad (9)$$

with $\tilde{\xi}_2$ and $\tilde{W}_2$ defined in (2) and the transition dipole moments $\tilde{D}_i$ to the channel basis function $\tilde{\Psi}_i$; $\tilde{\sigma}_{interloper}$ denotes the autoionizing cross-section of an interloper Rydberg series 2, which interacts with the open channels and acts as an envelope to the perturbed series; $\tilde{\varepsilon}_{1eff}$ and $\tilde{q}_{1eff}$ denote the reduced energy and the line profile index of the perturbed Rydberg series 1, respectively. This technique of separating the spectra of interlopers from single autoionizing Rydberg series has been extended to systems involving two autoionizing Rydberg series perturbed by interlopers, thus enabling the identification of the resonance structures of those systems.[9,10]

Unfortunately, the photoionization spectrum of molecular hydrogen considered by Jungen and Dill[17] does not belongs to either of the systems mentioned above. More than one interloper participates in channel coupling to perturb the autoionizing Rydberg series and the formulation previously developed for decomposing interlopers' spectra from autoionizing Rydberg series requires extending to be able to work with the effects of more than one interloper. First, restrict the formulation to a system in which two channels with higher ionization energies act as interlopers that perturb and one autoionizing Rydberg series. Extension to arbitrary numbers of interloper series will follow later.

Good Resonance Parameters. It is essential to have 'good' resonance parameters for the identification of resonance structures to describe scattering in perturbed autoionizing Rydberg series.[29-31] Pure resonance parameters relevant to the resonance positions and the widths uninfluenced by other dynamic factors, such as background scattering and avoided crossing interactions, can be obtained by considering the phase $\tilde{\delta}_r$ of the determinant of $\tan\tilde{\beta}+\tilde{\kappa}^{cc}$:[28] $\det(\tan\tilde{\beta}+\tilde{\kappa}^{cc})=C\exp(i\tilde{\delta}_r)$ where the complex reactance matrix $\tilde{\kappa}^{cc}$ denotes $\tilde{K}^{cc}-i\tilde{K}^{co}\tilde{K}^{oc}$ with $\Re(\tilde{\kappa}^{cc})=0$ or $\tilde{K}_{ii}=0$ ($i\in Q$) and C denotes the modulus of the determinant. Q denotes the set of closed channels. The phase shift $\tilde{\delta}_r$ is the shift caused by resonance scattering,[28] and is related to the reduced energy $\tilde{\varepsilon}_r$ by $-\cot\tilde{\delta}_r=\tilde{\varepsilon}_r$.

Now consider the decomposition of the cross section into terms corresponding to interlopers and autoionizing Rydberg series perturbed by them. For this, take indices 2 and 3 for the interloper series and index 1 for the perturbed autoionizing Rydberg series. The decomposition can be achieved by extracting $\begin{pmatrix}\tilde{\varepsilon}_2-i & \rho_{23}\\ \rho_{23} & \tilde{\varepsilon}_3-i\end{pmatrix}$ from $\det(\tan\tilde{\beta}+\tilde{\kappa}^{cc})$:[10,32]

$$\det(\tan\tilde{\beta}+\tilde{\kappa}^{cc})=\tilde{W}_1\tilde{W}_2\tilde{W}_3\begin{vmatrix}\tilde{\varepsilon}_1-i & \rho_{12} & \rho_{13}\\ \rho_{12} & \tilde{\varepsilon}_2-i & \rho_{23}\\ \rho_{13} & \rho_{23} & \tilde{\varepsilon}_3-i\end{vmatrix} \quad (10)$$

$$=\tilde{W}_1\tilde{W}_2\tilde{W}_3\begin{vmatrix}\tilde{\varepsilon}_2-i & \rho_{23}\\ \rho_{23} & \tilde{\varepsilon}_3-i\end{vmatrix}\left[\tilde{\varepsilon}_1-i-(\rho_{12}\ \rho_{13})\begin{pmatrix}\tilde{\varepsilon}_2-i & \rho_{23}\\ \rho_{23} & \tilde{\varepsilon}_3-i\end{pmatrix}^{-1}\begin{pmatrix}\rho_{12}\\ \rho_{13}\end{pmatrix}\right]$$

with ρ_{ij} denoting $\tilde{\kappa}_{ij}/(\tilde{\xi}_i\tilde{\xi}_j)$ whose real and imaginary parts are given by $(\tilde{K}_{ij}-i\tilde{\xi}_i\cdot\tilde{\xi}_j)/(\tilde{\xi}_i\tilde{\xi}_j)=\tilde{k}_{ij}-i$ for $i\neq j$ and $-i$ for $i=j$.

The interloper part can be expressed as

$$\begin{vmatrix}\tilde{\varepsilon}_2-i & \rho_{23}\\ \rho_{23} & \tilde{\varepsilon}_3-i\end{vmatrix}=(\tilde{\varepsilon}_{2s}+\tilde{\varepsilon}_{3s})(\tilde{\varepsilon}_{23}-i) \quad (11)$$

where $\tilde{\varepsilon}_{is}$ denotes $\tilde{\varepsilon}_i-\tilde{k}_{23}$ (i = 2, 3) and the reduced energy $\tilde{\varepsilon}_{23}$ of the coupled series is defined by

$$\tilde{\varepsilon}_{23}=\frac{\tilde{\varepsilon}_2\tilde{\varepsilon}_3-\tilde{k}_{23}^2}{\tilde{\varepsilon}_{2s}+\tilde{\varepsilon}_{3s}}. \quad (12)$$

The resonance behavior of the coupled series 2 and 3 is determined by the roots of $\tilde{\varepsilon}_2\tilde{\varepsilon}_3-\tilde{k}_{23}^2=0$ which is the condition for the bound states of systems only comprising two closed channels.[9,14] Consider the last bracket of Eq. (10). The negative of its imaginary part can be expressed as:

$$f_{1eff}=\frac{\tilde{W}_{1eff}}{\tilde{W}_1}=\frac{(\tilde{\varepsilon}_2\tilde{\varepsilon}_3-\tilde{k}_{23}^2-\tilde{\varepsilon}_2\tilde{k}_{13}-\tilde{\varepsilon}_3\tilde{k}_{12}+\tilde{k}_{12}\tilde{k}_{23}+\tilde{k}_{13}\tilde{k}_{23})^2}{(\tilde{\varepsilon}_2\tilde{\varepsilon}_3-\tilde{k}_{23}^2)+(\tilde{\varepsilon}_{2s}+\tilde{\varepsilon}_{3s})^2} \quad (13)$$

With the new parameter k_{1_23}

$$k_{1\_23}=\frac{\tilde{\varepsilon}_{2s}\tilde{k}_{13}+\tilde{\varepsilon}_{3s}\tilde{k}_{12}}{\tilde{\varepsilon}_{2s}+\tilde{\varepsilon}_{3s}} \quad (14)$$

Eq. (13) can be written as

$$f_{1\text{eff}} = \frac{(\tilde{\varepsilon}_{23} - k_{1\_23})^2}{\tilde{\varepsilon}_{23}^2 + 1} \tag{15}$$

Eventually the contents of the last bracket of (10) can be denoted as $f_{1\text{eff}}(\tilde{\varepsilon}_{1\text{eff}} - \text{i})$. The reduced energy of autoionizing series perturbed by interlopers is given by

$$\tilde{\varepsilon}_{1\text{eff}} = \frac{1}{f_{1\text{eff}}}(\tilde{\varepsilon}_1 - s_1) \tag{16}$$

where s_1 denotes the shift due to the perturbation by the interlopers

$$s_1 = (\tilde{\varepsilon}_{2s} + \tilde{\varepsilon}_{3s}) \frac{\left[\begin{array}{c}(2k_{1\_23} - \tilde{\varepsilon}_{23})(\tilde{\varepsilon}_{2s} + \tilde{\varepsilon}_{3s}) + (\tilde{k}_{12} - \tilde{k}_{13})^2 \\ -\tilde{\varepsilon}_{23}(2\tilde{k}_{12}\tilde{k}_{13}\tilde{k}_{23} - \tilde{\varepsilon}_3\tilde{k}_{12}^2 - \tilde{\varepsilon}_2\tilde{k}_{13}^2)\end{array}\right]}{(\tilde{\varepsilon}_{2s} + \tilde{\varepsilon}_{3s})^2 + (\tilde{\varepsilon}_2\tilde{\varepsilon}_3 - \tilde{k}_{23}^2)^2} \tag{17}$$

Substituting (13) and (16) into (10) yields

$$\begin{aligned}\left|\tan\tilde{\beta} + \tilde{\kappa}^{\text{cc}}\right| &= \tilde{W}_1\tilde{W}_2\tilde{W}_3(\tilde{\varepsilon}_{2s} + \tilde{\varepsilon}_{3s})(\tilde{\varepsilon}_{23} - \text{i}) f_{1\text{eff}}(\tilde{\varepsilon}_{1\text{eff}} - \text{i}) \\ &= \tilde{W}_2\tilde{W}_3(\tilde{\varepsilon}_{2s} + \tilde{\varepsilon}_{3s})(\tilde{\varepsilon}_{23} - \text{i})\tilde{W}_{1\text{eff}}(\tilde{\varepsilon}_{1\text{eff}} - \text{i})\end{aligned} \tag{18}$$

Decoupled Cross Section Formula. The final photoionization cross section formula is obtained as follows:

$$\sigma = K\tilde{\mathbf{D}}^2 = K(\tilde{D}^{\text{o}})^2 \frac{(\tilde{\varepsilon}_{23} + \tilde{q}_{23})^2}{\tilde{\varepsilon}_{23}^2 + 1} \frac{(\tilde{\varepsilon}_{1\text{eff}} + \tilde{q}_{1\text{eff}})^2}{\tilde{\varepsilon}_{1\text{eff}}^2 + 1} \tag{19}$$

The derivation of Eq. (19) starts with the form of the physical wavefunction given by[3]

$$\begin{aligned}\tilde{\Psi} &= \tilde{\Psi}^{\text{o}}\cos\tilde{\delta}_r + \tilde{\Psi}^{\text{c}}\cos\tilde{\beta}\tilde{Z}^{\text{c}} \\ &= \tilde{\Psi}^{\text{o}}\cos\tilde{\delta}_r - \tilde{\Psi}^{\text{c}}(\tan\tilde{\beta} + \tilde{K}^{\text{cc}})^{-1}\tilde{K}^{\text{co}}\cos\tilde{\delta}_r\end{aligned} \tag{20}$$

corresponding transition dipole moment is obtained as

$$\tilde{\mathbf{D}} = [\tilde{D}^{\text{o}} - \tilde{D}^{\text{c}}(\tan\tilde{\beta} + \tilde{K}^{\text{cc}})^{-1}\tilde{K}^{\text{co}}]\cos\tilde{\delta}_r \tag{21}$$

which can be expressed as

$$\tilde{\mathbf{D}} = \tilde{D}^{\text{o}}[D_{\text{cc}} + \tilde{\mathbf{q}}^{\text{c}} \cdot \text{cof}^{\text{cc}}(\tilde{W}^{\text{c}})^T] \frac{\cos\tilde{\delta}_r}{D_{\text{cc}}} \tag{22}$$

where D_{cc} denotes $\det(\tan\tilde{\beta} + \tilde{K}^{\text{cc}})$ and cof^{cc} is a $N_{\text{c}} \times N_{\text{c}}$ matrix whose (i, j)-th element is the cofactor given by $\text{cof}_{ij}(\tan\tilde{\beta} + \tilde{K}^{\text{cc}})$; $\tilde{\mathbf{q}}^{\text{c}}$ is the vector composed of $\tilde{q}_i = -\tilde{D}_i/(\tilde{D}^{\text{o}}\tilde{\xi}_i)$ $(i \in Q)$; $\text{cof}^{\text{cc}}(\tilde{W}^{\text{c}})^T$ is a vector. The content of the bracket of the right-hand side of (22) can be written as $(\tilde{\varepsilon}_{23} + \tilde{q}_{23})$ $(\tilde{\varepsilon}_{2s} + \tilde{\varepsilon}_{3s})$ $(\tilde{\varepsilon}_{1\text{eff}} + \tilde{q}_{1\text{eff}})$ where $\tilde{q}_{23}$ denotes the line profile index of the coupled interloper series 2 and 3 and is given by

$$\tilde{q}_{23} = \frac{\tilde{\varepsilon}_{2s}\tilde{q}_3 + \tilde{\varepsilon}_{3s}\tilde{q}_2}{\tilde{\varepsilon}_{2s} + \tilde{\varepsilon}_{3s}} \tag{23}$$

and $\tilde{q}_{1\text{eff}}$ denotes

$$\tilde{q}_{1\text{eff}} = \frac{1}{f_{1\text{eff}}}\left(s_1 + \tilde{q}_1 - \frac{1}{(\tilde{\varepsilon}_1 + \tilde{q}_1)(\tilde{\varepsilon}_{2s} + \tilde{\varepsilon}_{3s})}\left[\begin{array}{c}\tilde{\varepsilon}_2(\tilde{q}_1 + \tilde{k}_{13})(\tilde{q}_3 + \tilde{k}_{13}) \\ +\tilde{\varepsilon}_3(\tilde{q}_1 + \tilde{k}_{12})(\tilde{q}_2 + \tilde{k}_{12}) \\ -(\tilde{k}_{12} - \tilde{k}_{13})(\tilde{k}_{13}\tilde{q}_2 - \tilde{q}_3\tilde{k}_{12}) \\ -\tilde{k}_{23}\left[\begin{array}{c}(\tilde{q}_1 + \tilde{k}_{13})(\tilde{q}_2 + \tilde{k}_{12}) \\ +(\tilde{q}_1 + \tilde{k}_{12})(\tilde{q}_3 + \tilde{k}_{13})\end{array}\right]\end{array}\right]\right) \tag{24}$$

Note that $\tilde{q}_{1\text{eff}}$ has poles at the zeros of $f_{1\text{eff}}$ and at $\tilde{\varepsilon}_{23} + \tilde{q}_{23} = 0$ and that we obtain

$$\frac{\cos\tilde{\delta}_r}{D_{\text{cc}}} = \frac{1}{C} = \frac{1}{\tilde{W}_{1\text{eff}}\tilde{W}_2\tilde{W}_3\left|\tilde{\varepsilon}_{2s} + \tilde{\varepsilon}_{3s}\right|[(\tilde{\varepsilon}_1^2 + 1)(\tilde{\varepsilon}_{1\text{eff}}^2 + 1)]^{1/2}} \tag{25}$$

Inserting (25) into (22), we finally obtain

$$\tilde{\mathbf{D}}^2 = (\tilde{D}^{\text{o}})^2 \frac{(\tilde{\varepsilon}_{23} + \tilde{q}_{23})^2}{\tilde{\varepsilon}_{23}^2 + 1} \frac{(\tilde{\varepsilon}_{1\text{eff}} + \tilde{q}_{1\text{eff}})^2}{\tilde{\varepsilon}_{1\text{eff}}^2 + 1} \tag{26}$$

Resonance Structures in Auto-ionizing Series of Hydrogen Molecules

Let us apply the above formulation to the resonance structures of the ro-vibrational pre-ionization spectra of H_2 studied by Jungen and Dill[17] using the frame transformation version of MQDT. The study of Jungen and Dill remains one of the most accurate and extensive studies, reproducing the measurements of Dehmer and Chupka[13] quite well (see Fig. 6 of Ref. 17). We want to supplement their study through the use of phase-shifted MQDT in which the resonance structures are transparently identified. Before examining resonance structures further, let us describe frame-transformation MQDT first using the H_2 system as an example.

The simplest resonance structure in the photoionization spectra of H_2 is the rotational preionization occurring at energies between the $N^+ = 0$ and 2 rotational thresholds pertaining to $H_2^+ {}^2\Sigma_g^+$, $v^+ = 0$ in the photoionization of H_2 X $^1\Sigma_g^+$ $(J'' = 0,\ v'' = 0)$.[15] In this energy range, the channel pertaining to the lowest ionization threshold ($N^+ = 0$) is open and the one pertaining to the next lowest ionization threshold is closed, yielding an autoionizing Rydberg series. The other closed channels act as interlopers to the autoionizing series. Let the energy range be such that the effects of the interlopers can be ignored and only channel coupling between the open channel corresponding to $(v^+, N^+) = (0, 0)$ and the rotationally preionizing channel corresponding to (0, 2) needs to be considered. For rotational pre-ionization to occur, the Rydberg electron should take the rotational energy $6B$ from the ionic core, which is possible only at the short-range over which it can interact strongly with the ionic core.

Fano noted[15] that electronic states are described by Born-Oppenheimer states or by the Hund case (b) at short-range, while they are described by l uncoupling states at long-range or by Hund case (d). Strong channel coupling at short range affects the photoionization spectra only through energy-insensitive quantum defect theory (qdt) parameters, allowing us to replace strong coupling by a few energy-insensitive qdt parameters. However, the qdt parameters of short-range dynamics cannot be directly used for long-range analysis because of the prevalence of different eigen-frames at short- and long- ranges. To use short-range qdt parameters at long range, frame-transformation matrices $\langle\Lambda|N^+\rangle$ from the Born-Oppenheimer states $|\Lambda\rangle$ to the l uncoupling states $|N^+\rangle$ should be considered.[15] For rotational preionization, the vibrational motions of nuclei are not included; only the frame transformation of the rotational part is involved and an

analytical formula can be obtained.[15] If vibrational preionization is considered, the corresponding frame transformation is the scalar product $\langle R|v^+\rangle$ of the vibrational states $|v^+\rangle$ and the position vector $|R\rangle$. Overall, the frame transformation matrix becomes $\langle R\Lambda|v^+N^+\rangle$ or $\langle R\Lambda|i\rangle$ with $|i\rangle \equiv |v^+N^+\rangle$.

Using this, now consider the effects of interlopers. In the spectral range between two rotational thresholds corresponding to $N^+ = 0$ and 2 pertaining to the $^2\Sigma_g^+$ $v^+ = 0$ state of H_2^+ in the photoionization of H_2 X $^1\Sigma_g^+$ ($J'' = 0$, $v'' = 0$), channels pertaining to the thresholds $v^+ > 0$ enter as interlopers and cause vibrational preionization. To obtain convergence, Jungen and Dill included twenty-two channels with cores corresponding to the states of H_2^+ specified with v^+ from 0 to 10 for each $N^+ = 0$ and 2. Convergence can be tested by the unitarity of the frame transformation matrix $\langle \Lambda R|v^+N^+\rangle^{J'}$ (the super-index J' denotes the total angular moment quantum number). This was confirmed to 6 significant figures in the 22-channel calculation by obtaining vibrational wavefunctions using the De Vogelaere algorithm[33] for propagation and shooting at both ends and matching in the middle. We used the electronic potential of the $^2\Sigma_g^+$ $v^+ = 0$ state of H_2^+ obtained by Wind,[34] complemented by the adiabatic correction of Beckel, Hansen and Peek.[35] Vibrational wavefunctions thus obtained by us can be found in the submitted supplementary materials. However, the deviation of $\Sigma_{i'',\Lambda,\Lambda'}\langle i|\cos\pi\mu_\Lambda|i''\rangle\langle i''|\cos^{-1}\pi\mu_{\Lambda'}|i'\rangle$ from $\delta_{ii'}$ is not negligible in the highly excited vibrational states. The number of corresponding significant figures decreases from 6 to 3 when v^+ increases from 0 to 10. Because of this deviation, $\langle i|\tan\pi\mu_\Lambda|i'\rangle$ obtained by $\Sigma_{i'',\Lambda,\Lambda'}\langle i|\sin\pi\mu_\Lambda|i''\rangle\langle i''|\cos^{-1}\pi\mu_{\Lambda'}|i'\rangle$ is not symmetric.[19] In contrast, the spectrum itself converges at a much smaller number of channels,[24] indicating the sufficiency of 22 channels.

The involvement of so many vibrational states is explained by the Franck-Condon factor (Table 1), which decreases slowly with increasing vibrational quantum number. This slow convergence is caused by the shift of the potential minimum of H_2^+ to larger inter-nuclear distances. This contrasts greatly with the spectrum obtained by Xu *et al.*,[20] in which the $E, F\ ^1\Sigma_g^+$ states are used as intermediates whose

Table 1. Franck-Condon factors $\langle v^+N^+H_2^+X^2\Sigma_g^+|v''=0, J''=0\ H_2X^1\Sigma_g^+\rangle$

v^+	N^+	
	0	2
0	0.3008	0.2922
1	0.3995	0.3916
2	0.4167	0.4121
3	0.3905	0.3891
4	0.3456	0.3469
5	0.2963	0.2994
6	0.2496	0.2538
7	0.2084	0.2131
8	0.1734	0.1783
9	0.1443	0.1490
10	0.1203	0.1248

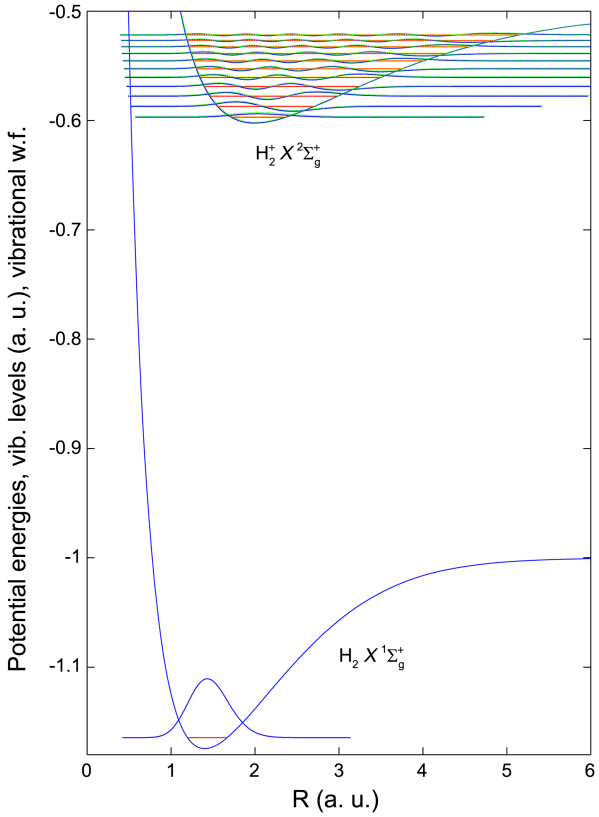

Figure 2. Potential energy curves, vibrational energy levels, and wavefunctions for the $v'' = 0$, $J'' = 0$ state of H_2 X $^1\Sigma_g^+$ and $v^+ = 0$-10, $N^+ = 0$, 2 states of H_2^+ X $^2\Sigma_g^+$. The $N^+ = 0$ and 2 cases are discernible only with great care.

equilibrium nuclear distances are close to that of H_2^+. The participating number of closed channels is much smaller in this case. For convenience, 22 channels will be indexed from $i = 1$ to 22 as follows. Let the channels for v^+ from 0 to 10 with $N^+ = 0$ be indexed by $i = 1, 3, ..., 21$. Likewise, the channels for v^+ from 0 to 10 with $N^+ = 2$ are indexed by $i = 2, 4, ..., 22$. The open channel corresponds to $i = 1$. The perturbed autoionizing series corresponds to the Rydberg series belonging to $i = 2$. The interloper series belong to the remaining $i = 3,..., 22$.

Autoionization spectra can be analyzed using phase-shifted MQDT by first setting diagonal elements of the reactance matrix to zero. Making diagonal elements zero can be obtained by solving the coupled equations (3)-(6) for μ_i. The supplementary materials contain the reactance matrix thus obtained and other qdt parameters used to obtain it. Using this tilde reactance matrix allows analysis of the resonance structures of the rotational preionization perturbed by interlopers. As mentioned above, all 22 channels need not be included to achieve convergent calculation of the photoionization cross section σ. Convergence can almost be obtained with only 8 channels; 12 channels are enough (Fig. 3). This rapid convergence of the photoionization spectrum can be explained[24] by the rough linearity of the quantum defect functions $\mu_\Lambda(R)$ near $R=R_e$ and the approximately harmonic nuclear motion. The four channel calculation for

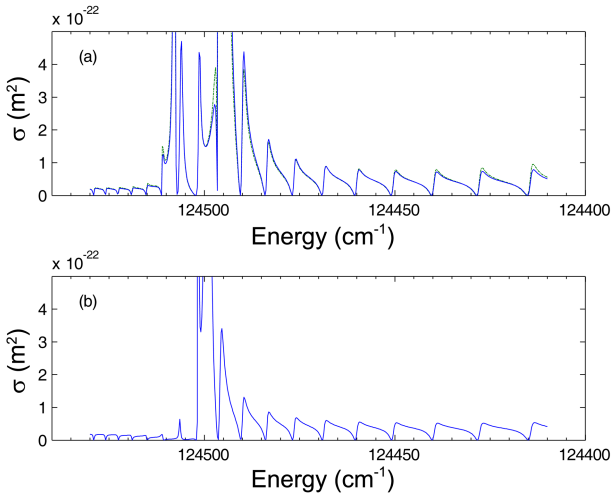

Figure 3. (a) 22- (dash-dot) and 8- (solid) channel calculations of the autoionization spectrum. They are noticeably different only at around 124500 cm^{-1}. (b) 4-channel calculation of the autoionization spectrum.

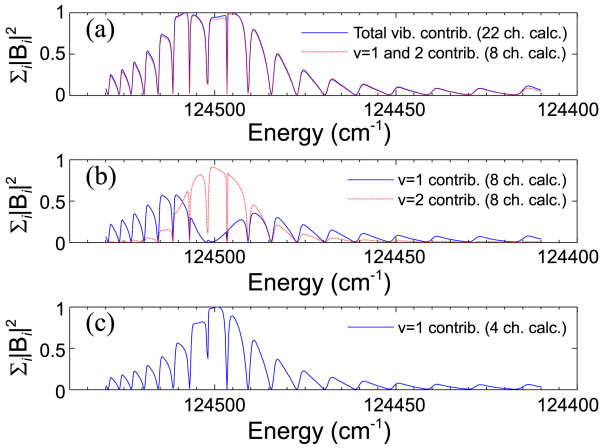

Figure 4. (a) Comparison of the sum of the vibrational contributions $v = 1$ to 10 of the 22-channel calculation and the sum of the $v = 1$ and 2 contributions of the 8-channel calculation. (b) The separate contributions of $v = 1$ ($\Sigma_{i=3}^{4}|B_i|^2$) and $v = 2$ ($\Sigma_{i=5}^{6}|B_i|^2$) in the 8-channel calculation. (c) The contribution of $v = 1$ ($\Sigma_{i=3}^{4}|B_i|^2$) in the 4-channel calculation. $i = 3$ is for $v^+ = 1$ and $N^+ = 0$, $i = 6$ is for $v^+ = 2$ and $N^+ = 2$ and so on.

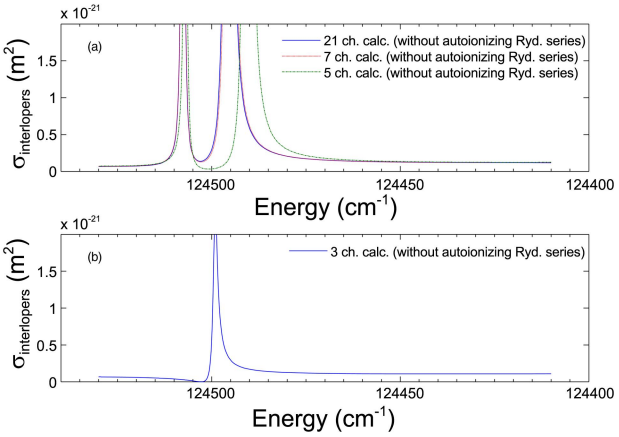

Figure 5. Interloper spectra excluding the autoionizing Rydberg series (channel 2). (a) The 7-channel calculation closely followed the 21-channel calculation. The two peaks correspond to 7pπ $v = 1$ and 5pπ $v = 2$ peaks. (b) Only a single peak (7pπ $v = 1$) appears in the 3 channel calculation.

which the explicit formula is given deviates markedly from the 22-channel calculation around the resonance peaks of interloper series, although they converge at energies far from the resonance peaks of interloper series. This deviation is expected since the interloper spectrum is caused not only by $v^+ = 1$ channels but also by those of $v^+ = 2$. In the 4 channel calculation, only $v^+ = 1$ channels are considered in the interloper spectrum (two $v^+ = 0$ and two $v^+ = 1$ channels comprise 4 channels).

Although only the ground vibrational state ($v^+ = 0$) is observed in the H_2^+ molecular ion at the energy range in Figure 3, vibrationally excited states of the H_2^+ core ion participate in photoionization at short and intermediate radial ranges. Contributions of vibrationally excited states ($v^+ > 0$) can be examined by calculating the squares of the moduli of the expansion coefficients B_i of $\tilde{\Psi}=\Sigma_i\tilde{\Psi}_iB_i$. Plots of the whole contribution of the $\Sigma_{i=3}^{10}|B_i|^2$ vibrationally excited channels obtained from the 22 channel calculation and the contribution from only the $v^+ = 1$ and 2 channels obtained from the 8 channel calculation (Fig. 4(a)) show that contributions of vibrationally excited channels are not localized around the interloper peak. They are delocalized over the whole energy range of the spectrum, though their contributions are most prominent around the interloper peak. $v^+ = 1$ and 2 contributions comprise most of the contributions of the vibrationally excited channels despite v^+ up to 10 being needed for convergence in the frame transformation matrix. The central resonance peak around 124500 cm^{-1} has contributions mostly from $v^+ = 2$ (Fig. 4(b)). This central peak remains if $v^+ = 2$ channels are excluded from the calculation (Fig. 4(c)), indicating that the $v^+ = 1$ contribution is suppressed at the central peak when there are $v^+ = 2$ channels but becomes free and contributes to the central peak when $v^+ = 2$ channels disappear.

The central peak is sensitive to the number of participating interloper channels (Fig. 3), i.e. it is sensitive to the structured background (or structured continuum) produced by the interloper channels. Consider the structured continuum alone. It can be obtained simply by excluding the perturbed autoionizing series, i.e., the $i = 2$ channel from the calculation.

The structured background spectra for 5-, 7- and 21-channel systems (Fig. 5) show that resonance peak positions move as number of interloper channels varies from 3 to 7. Even two interloper series in the 3-channel calculation greatly interact with each other. Resonance peak position is greatly shifted from the unperturbed peak position (Fig. 6), something rarely observed in atomic spectra. It derives from the strong rotational coupling in H_2 between the channels pertaining to $N^+ = 0$ and 2 with the same v^+.

Decomposing the spectrum into interloper and perturbed autoionizing Rydberg parts (Fig. 7(a)) shows that it is

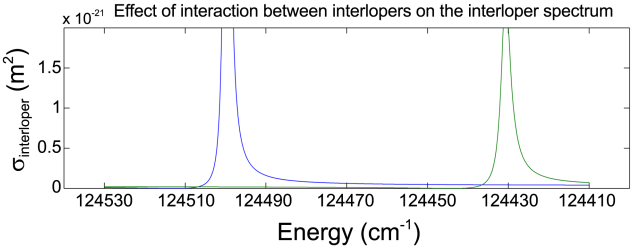

Figure 6. The 7pπ v =1 peak located at ~124430 cm^{-1} belonging to channel 4 is greatly shifted to ~124500 cm^{-1} upon channel coupling with channel 3. The new peak position can be obtained by the bound energy calculation including only closed channels 2 and 3 and solving the bound condition $\tilde{\varepsilon}_2\tilde{\varepsilon}_3-\tilde{k}_{23}^2=0$.

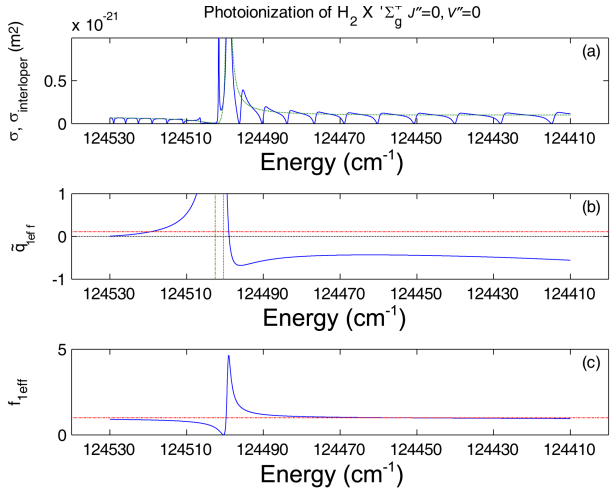

Figure 7. Preionization spectrum obtained by 4 channel QDT. (a) The cross section is drawn with a solid line, that of the interlopers served as an envelope (dashed line). (b) The line profile index for the autoionizing Rydberg series perturbed by interloper series. The unperturbed profile $\tilde{q}_1$ is also shown (dash-dotted line). The two vertical lines denote the positions of simple poles corresponding to $\tilde{\varepsilon}_{23}=-\tilde{q}_{23}$ (left) and $\tilde{\varepsilon}_{23}=\tilde{k}_{1\_23}$ (right). (c) The reduced width of the perturbed autoionizing Rydberg series. The dash-dotted line located at $f_{1\text{eff}}=1$ is the unperturbed value of $f_{1\text{eff}}$.

enveloped by the interlopers' spectrum and chopped by the rotationally preionizing Rydberg series. The Fano's line profile function $\tilde{q}_{1\text{eff}}$ for the preionizing Rydberg series perturbed from its unperturbed $\tilde{q}_1$ by interlopers (Fig. 7(b)) shows two reversals of sign q. The sign of $\tilde{q}_{1\text{eff}}$ determines the direction of the asymmetry of the resonance peaks.[36] The factor $\tilde{q}_{1\text{eff}}^2+1$ serves as an enhancement factor[30] due to channel coupling and is close to unity since $\tilde{q}_{1\text{eff}}$ is smaller than 1 for most of the spectral range (Fig. 7(b)) except around 124500 cm^{-1}, where two simple poles $\tilde{\varepsilon}_{23}=\tilde{k}_{1\_23}$ and $\tilde{\varepsilon}_{23}=-\tilde{q}_{23}$ are located. Although perturbation due to channel does not cause much spectral enhancement, the shape of the autoionizing Rydberg series spectrum is very different from that of the unperturbed spectrum at all energies. This contrasts with the behavior of the spectral width $\tilde{W}_1 f_{1\text{eff}}$ of the autoionizing Rydberg series (Fig. 7(c)). $f_{1\text{eff}}$ remains close to the unperturbed value of 1 over almost all the energy range. The strong perturbation around 124500 cm^{-1} occurs at $\tilde{\varepsilon}_{23}=\tilde{k}_{1\_23}$ where the zero of the reduced spectral width $\tilde{W}_1 f_{1\text{eff}}$ occurs.

Extension of the Formulation to Arbitrary Numbers of Interloper Channels

The formulation (10) to (26) is for 3 closed channels of which 2 are interlopers. According to the previous sections, for the analysis to be meaningful, there should be no limit to the number of interloper channels in the formulation. Consider the extension of the formulation (10)-(26) to an arbitrary number of interloper channels to isolate the interloper's spectrum from the perturbed autoionizing Rydberg series as in Eq. (26). For the arbitrary number of interloper channels, the notation of $\tilde{\varepsilon}_{23}$ and $\tilde{q}_{23}$ in Eq. (26) need to become $\tilde{\varepsilon}_{\text{I}}$ and $\tilde{q}_{\text{I}}$, respectively, to indicate that there are now more interloper series than 2 or 3 so that Eq. (26) becomes

$$\tilde{\mathbf{D}}^2=(\tilde{D}^{\text{o}})^2\frac{(\tilde{\varepsilon}_{\text{I}}+\tilde{q}_{\text{I}})^2}{\tilde{\varepsilon}_{\text{I}}^2+1}\frac{(\tilde{\varepsilon}_{1\text{eff}}+\tilde{q}_{1\text{eff}})^2}{\tilde{\varepsilon}_{1\text{eff}}^2+1} \tag{27}$$

Obtaining formulas for $\tilde{\varepsilon}_{\text{I}}$ and $\tilde{q}_{\text{I}}$ and subsequently for $\tilde{\varepsilon}_{1\text{eff}}$ and $\tilde{q}_{1\text{eff}}$ is difficult. This study adopts a different strategy. Their formulas are temporarily derived to calculate their values during the calculation at each energy point by the symbolic operation available in MATLAB®. The derived formulas are too complex to be practically hard-coded, necessitating their repeated symbolic derivation at every energy point. Using the determinant identity $|A| = |B||E-DB^{-1}C|$ for $A=\begin{pmatrix} B & C \\ D & E \end{pmatrix}$, $|\tilde{\varepsilon}+\rho|$ can be decomposed into the terms for the interloper and perturbed series:

$$|\tilde{\varepsilon}+\rho|=|\tilde{\varepsilon}^{\text{I}}+\rho^{\text{I}}||\tilde{\varepsilon}_{\text{I}}+\rho_{\text{I}}-\rho^{\text{pI}}(\tilde{\varepsilon}^{\text{I}}+\rho^{\text{I}})^{-1}\rho^{\text{Ip}}| \tag{28}$$

The term $|\tilde{\varepsilon}^{\text{I}}+\rho^{\text{I}}|$ for the interlopers can be expressed as $\Im(|\tilde{\varepsilon}^{\text{I}}+\rho^{\text{I}}|)(\tilde{\varepsilon}_{\text{I}}-\text{i})$ from which $\tilde{\varepsilon}_{\text{I}}$ is obtained. The term $|\tilde{\varepsilon}_{\text{I}}+\rho_{\text{I}}-\rho^{\text{pI}}(\tilde{\varepsilon}^{\text{I}}+\rho^{\text{I}})^{-1}\rho^{\text{Ip}}|$ for the perturbed series p can be written as $f_{1\text{eff}}(\tilde{\varepsilon}_{1\text{eff}}-\text{i})$ from which $f_{1\text{eff}}$ and $\tilde{\varepsilon}_{1\text{eff}}$ can be obtained. The shift s_1 can be obtained by expressing $\tilde{\varepsilon}_{1\text{eff}}$ into

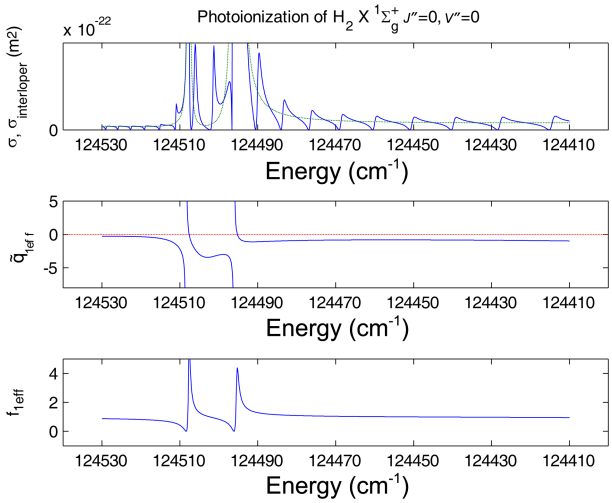

Figure 8. A similar analysis to that of Figure 7 but with 6 interloper series.

the form of (16). The line profile function $\tilde{q}_I$ for the interloper spectrum is obtained by first obtaining the coefficient of $\tilde{\varepsilon}_I$ for the bracketed term of (22) and then subtracting $\tilde{\varepsilon}_I$ from the coefficient. Substituting $\tilde{\varepsilon}_{1\text{eff}}$, s_1, $\tilde{\varepsilon}_I$, and $\tilde{q}_I$ into (22), $\tilde{q}_{1\text{eff}}$ can be finally obtained. This procedure can be coded by MATLAB®'s symbolic operation. Decomposition of the cross section into Eq. (27) is possible by this on-the-fly derivation (Fig. 8), though it is too time-consuming to be used practically. This section, however, demonstrates that this type of analysis, based on decomposing the resonance structures, can be performed for arbitrary numbers of interloper series. If general formulas that can be hardcoded are derived for the arbitrary number of interloper series, computing time will be greatly reduced and analyses of pole structures will become practicable.

Results and Discussion

The preionization spectrum of H_2 in the region immediately above the ionization threshold of H_2^+ ($^2\Sigma_g^+$, $v^+ = 0$, $N^+ = 0$) converging toward its rotationally excited ($v^+ = 0$, $N^+ = 2$) limit is perturbed by two vibrationally excited levels 7pπ $v = 1$ and 5pπ $v = 2$. The spectrum may be expected to be described by a system comprising 2 interlopers and one autoionizing Rydberg series perturbed by them. A formulation that can analyze the resonance structures of a four channel system composed of 1 open, 2 interloper, and 1 autoionizing Rydberg channels is developed here since no previous formulation is available. It is then applied to the preionization spectrum of H_2.

Unlike the expectation that two interloper series can describe the two interloper peaks assigned to 7pπ $v = 1$ and 5pπ $v = 2$, the formulation that includes only two interloper channels cannot describe the spectrum. This was attributable to the strong rotational coupling in H_2 that led to the two rotational channels pertaining to $N^+ = 0$ and 2 being included in the channel coupling for a given vibrational quantum number. This increased the minimum number of channels to 6 to allow reproduction of the rotational preionization spectrum of H_2 perturbed by 7pπ $v = 1$ and 5pπ $v = 2$. However, the spectrum generated using 6 channels remained different from that observed experimentally. Using at least 8 channels allowed satisfactory reproduction of the experimental data. To be able to model the effects of more than 2 interloper series, the symbolic operation functionality of MATLAB® was used to derive formulas on the fly for each energy point. This approach allowed the decomposition of the interlopers' spectrum from the perturbed autoionizing Rydberg spectrum for the system involving 8 channels. However it is very time-consuming and since the temporary formulas are too complicated to be written down, its use is limited to calculational purposes and it cannot be used to analyse pole structures. Therefore its use is very limited. Deriving explicit formulas for arbitrary numbers of interlopers would greatly aid the process and will constitute future research.

Although the formulation for two interlopers could not reproduce the observed spectrum, it guided the symbolic derivation of the formulas that could. It also has the potential to guide other future general formulations. There are also several dynamic aspects of the spectrum that are independent of the number of interloper series and thus can be studied with this limited formulation. Vibrational preionization in the H_2 spectrum is not localized near the resonance peaks due to interlopers but is delocalized over the spectrum's whole energy range, something not common in other systems. It is likely related to the strong rotational channel coupling, given that the position of the quasi-bound state of the coupled interlopers 2 and 3 is shifted greatly from the unperturbed bound state of interloper 3.

To reproduce satisfactorily the spectrum, vibrational channels up to $v = 5$ were found to be needed. Although the $v = 3$, 4 and 5 vibrational channels are needed to achieve a satisfactory spectrum, they showed negligible contributions at short- and intermediate-range, measured by the normalized B_i^2 ($i = 3$, 4, 5). The local and nonlocal behaviors of dynamic parameters are also interesting. The shapes of the spectral lines of the autoionizing Rydberg series are affected by interlopers over the whole energy range, though the reduced spectral widths of the perturbed autoionizing Rydberg series are only affected over a narrow range.

Acknowledgments. This study was supported by an Ajou University Research Fellowship of 2011 and the Basic Science Research Program through the National Research Foundation of Korea (NRF) funded by the Ministry of Education, Science and Technology (2011-0024808).

References

1. Aymar, M.; Greene, C. H.; Luc-Koenig, E. *Rev. Mod. Phys.* **1996**, *68*, 1015.
2. Giusti-Suzor, A.; Fano, U. *J. Phys. B* **1984**, *17*, 215.
3. Fano, U.; Rau, A. R. P. *Atomic Collisions and Spectra*; Academic: Orlando, U.S.A., 1986.
4. Cooke, W. E.; Cromer, C. L. *Phys. Rev. A* **1985**, *32*, 2725.
5. Ueda, K. *Phys. Rev. A* **1987**, *35*, 2484.
6. Connerade, J. P. *Proc. R. Soc. London, Ser. A* **1978**, *362*, 361.
7. Lane, A. M. *J. Phys. B* **1984**, *17*, 2213.
8. Fano, U.; Cooper, J. W. *Phys. Rev.* **1965**, *137*, A1364.
9. Lee, C.-W.; Kim, J.; Gim, Y.; Lee, W.-J. *J. Phys. B* **2011**, *44*, 065002.
10. Lee, C.-W. *J. Phys. B* **2011**, *44*, 195005.
11. Kalyar, M. A.; Rafiq, M.; Baig, M. A. *Phys. Rev. A* **2009**, *80*, 052505.
12. De Graaff, R. J.; Ubachs, W.; Hogervorst, W.; Abutaleb, M. *Phys. Rev. A* **1990**, *42*, 5473.
13. Dehmer, P. M.; Chupka, W. A. *J. Chem. Phys.* **1976**, *65*, 2243.
14. Giusti-Suzor, A.; Lefebvre-Brion, H. *Phys.Rev. A* **1984**, *30*, 3057.
15. Fano, U. *Phys. Rev. A* **1970**, *2*, 353.
16. Atabek, O.; Dill, D.; Jungen, C. *Phys. Rev. Lett.* **1974**, *33*, 123.
17. Jungen, C.; Dill, D. *J. Chem. Phys.* **1980**, *73*, 3338.
18. Greene, C. H.; Jungene, C. *Adv. At. Mol. Phys.* **1985**, *21*, 51.
19. Bjerre, N.; Kachru, R.; Helm, H. *Phys. Rev. A* **1985**, *31*, 1206.
20. Xu, E. Y.; Helm, H.; Kachru, R. *Phys. Rev. A* **1989**, *39*, 3979.
21. Fielding, H. H.; Softley, T. P. *Phys. Rev. A* **1994**, *49*, 969.
22. Du, N. Y.; Greene, C. H. *J. Chem. Phys.* **1986**, *85*, 5430.
23. Jungen, C.; Raoult, M. *Faraday Discuss Chem. Soc.* **1981**, *71*, 253.
24. Raoult, M.; Jungen, C. *J. Chem. Phys.* **1981**, *74*, 3388.

25. Kirrander, A.; Jungen, C.; Fielding, H. H. *Phys. Chem. Chem. Phys.* **2010**, *12*, 8948.
26. Lecomte, J. M. *J. Phys. B* **1987**, *20*, 3645.
27. Lee, C.-W.; Kim, J.-H. *Bull. Korean Chem. Soc.* **2002**, *23*, 1560.
28. Lee, C.-W. *Bull. Korean Chem. Soc.* **2009**, *30*, 891.
29. Lee, C.-W. *Bull. Korean Chem. Soc.* **2010**, *31*, 3201.
30. Cho, B.; Lee, C. W. *Bull. Korean Chem. Soc.* **2010**, *31*, 315.
31. Lee, C.-W. *Bull. Korean Chem. Soc.* **2010**, *31*, 1669.
32. Zwillinger, D.; 30th ed.; C R C Press: Boca Raton, 1996.
33. Lester, W. A., Jr. *J. Comput. Phys.* **1968**, *3*, 322.
34. Wind, H. *J. Chem. Phys.* **1965**, *42*, 2371.
35. Beckel, C. L.; Hansen, B. D.; Peek, J. M. *J. Chem. Phys.* **1970**, *53*, 3681.
36. Fano, U. *Phys. Rev.* **1961**, *124*, 1866.